DYNAMIC ANALYSIS OF SLENDER COLUMNS UNDER SELF-WEIGHT USING DIGITAL IMAGE PROCESSING TECHNIQUES

Daniel Leonardo Braga Rodriguez Jurjo
Carlos Magluta
Ney Roitman
Civil Engineering Program, COPPE/UFRJ, PO BOX: 68506, Rio de Janeiro, RJ, Brazil
jurjo@coc.ufrj.br

Abstract. *This paper presents an experimental methodology developed to obtain the dynamic responses of structures that cannot be monitored by conventional sensors, based on the digital image processing techniques. The importance of this methodology is to perform large displacements measurement without making contact with the structure, therefore, not introducing undesirable modifications in the behavior of the structure. In order to verify the applicability of the experimental methodology, a clamped-free column under self-weight made of a thin-walled sheet of brass was experimentally analyzed. The theoretical and experimental results were compared. In this experimental analysis the natural frequencies and the damping ratios for the first normal mode of vibration for different column lengths were obtained. Performed in order to study the behavior of the dynamic properties in two different configurations of the column: compressed and tensioned. The natural frequencies obtained experimentally were consistent with the theoretical results, confirming the accuracy and versatility of the present methodology.*

Keywords*: Image Processing, Large Displacements, Self-Weight, Experimental Analysis*

1. Introduction

The use of reduced scale models in experimental analysis has as a main objective to provide knowledge about the behavior of the actual structure, for example, in the oil industry, where the increasing need of perforation of oil in deep and ultra deep waters implies the development of extremely reduced models, despite the great inherent dimensions of the test tanks. However, the analysis related to the behavior of these structures using conventional sensors became impracticable, since the mass of the sensors could have modified the behavior of the models. Consider, for example, the case of a reduced model of a riser with diameter of 10" in a 1/100 scale. This would imply a model with a diameter of 0.1". It is clear that for this model the conventional sensors would completely modify the behavior of the structure. Therefore, there is an increasing interest in developing alternative forms to measure movements without making contact with the structure, allowing reliable analyses about the displacements suffered by such structures.

In this study, an experimental methodology was developed, allowing the measurement of static and dynamic displacements without making contact with the structure, using digital image processing techniques. This methodology uses only adhesive markers of negligible mass in relation to the structure, facilitating the accomplishment of the instrumentation for the experimental assay. Besides the scale reduced models, this methodology can also be applied to great civil structures, such as: bridges, viaducts, etc., where it is difficult to obtain a reference to use the conventional displacement sensors.

Image processing is a very useful tool that provides objective results in an entirely automatic way. The techniques of image processing have evolved very rapidly due to the increasing power of personal computers, image capturing systems and to the development of algorithms and softwares. These techniques find applications in fields such as measurement of displacements in structures (Jurjo, 2004a; Jurjo, 2004b), morphological information to understand the behavior of a material, medical diagnosis, three-dimensional kinetic analysis of human movements (Barros *et al*.,1994), production lines and robotics. The image processing has as its main objectives, to improve the quality and to enhance aspects of interest in the digital image, aiming to extract useful information that helps the process of analysis.

With the purpose of testing the viability of the present methodology, an experimental dynamic analysis of a clamped -free column under self-weight made of a thin-walled sheet of brass was conducted. As this kind of structure presents a high index of slenderness, its answers could be affected by the introduction of conventional sensors.

This experimental methodology was applied in a computational vision system that integrates on-line the acquisition of the image, the processing through special programming routines and the identification of points of interest (adhesive markers).

In this methodology, there are two important processes: calibration and reconstruction. In the calibration process, the image coordinates (u,v) of the points and their respective real coordinates (x,y,z) are known. The purpose of this process is to get the transformation matrix using these two sets of coordinates. The transformation matrix establishes the correlation between the real and the image coordinates. The reconstruction process consists in knowing the transformation matrix and the coordinates of the image, to obtain the real coordinates.

Using these two processes, the values of the real displacements suffered by the structures can be obtained from its respective values in pixels in the image, allowing the measurements of the displacements without making contact with the structure.

To assure the accuracy and the applicability of the present methodology, the experimental and theoretical results were compared.

2. Experimental Methodology

The experimental methodology developed in this study is composed by the three following stages:

(i) In the first stage, there's the capture of the images performed by an analogical video camera with NTSC system and CCD of ¼ inch, with a total of 811(H) x 508 (V) CCD pixels. The camera presents a scanning system of 525 lines with 60 frames/second, resolution of 470 TV Lines, electronic shutter with 1/120000 seconds, manual and automatic focus, Cannon lenses with 22X of optical zoom and 220X of digital zoom and focal distance varying from 3.7 to 85.1 mm. The dimensions of the camera are: 77x50x60 mm.

(ii) In the second stage, the conversion of the analogical images to digital images is performed, using a monochromatic frame grabber (PCI-1409/National Instruments) inserted in the personal computer.

(iii) In the third stage, which is the most important one, the acquisition and the processing of the digital images is done, with the objective of preparing them for the calibration and the reconstruction processes, allowing the determination of the dynamic displacements in the columns.

From these stages, it was possible to develop a computational vision system based on the programming language LabVIEW (version 6.1-National Instruments), which received the name Image-Sensor Program (ISP).

In the ISP, the processing routine consists of cutting the interest area in the image, allowing to decrease the time of processing and the noises that are outside the analysis area, threshold it, turn gray level images into binary ones to enhance the interest points, and later, to identify the coordinates (u,v) of these points.

The computation of coordinates u and v of the interest points in the image is made by transforming these points into small regions of interest, known in image processing as ROI (Regions of Interest). The ROI is characterized by a register (data set) that contains the contour coordinates of a determined region.

The interest points can be converted into ROIs by launching a "mask" onto the binary image. In the binary image only the interest points are in white color and the background in black color. Thus, the mask gets to identify each one of the regions, looking for the borders coordinates between black and white pixels. With the coordinates of the borders it is possible to determine the central coordinates of each one of the regions. One of the main advantages of this process is that it can be performed with a great efficiency, generating a low computational cost. Another advantage is associated with the small number of information which has to be stored for each one of the images acquired along the time.

In order to have this system working properly, the acquisition and processing routines in the ISP are executed in parallel. Thus, while the acquisition routine waits and digitizes an image, the processing routine segments (threshold), identifies and calculates the coordinates (u,v) of the interest points in the last digitized image.

The calibration is performed by identifying the coordinates u and v of the selected calibration points in the image by inserting their respective real coordinates (x and y (2D) or x, y and z (3D)), which are previously known. This process is done by the calibration routine in the ISP. The selection of the calibration points in the image is performed by the mouse. After this selection, the values of the image coordinates are inserted automatically in a collection box by the ISP. The real coordinates are typed in this same box.

To obtain the transformation matrix, which establishes the correlation between the real and the image coordinates, it is necessary to apply a suitable calibration method. There are several methods of calibration, being the most used the following ones: Direct Linear Transformation (DLT) (Abdel-Aziz and Karara, 1971; Chen *et al*., 1994) and Tsai (Tsai, 1986). The method chosen for this study was the standard DLT, by virtue of the minimum level of distortions caused by the lenses of the video camera.

2.1. Calibration Method

The DLT method is based on the underlying ideas of the analytic photogrammetry, which has as its main objective to provide information about position, orientation and dimensions of objects in the space from the stereoscopic registers of its projections in images. The analytic photogrammetry is mainly based on the called "Basic Equation of the Photogrammetry" or "Collinearity Equation" (Haralick and Shapiro, 1993). This equation shows that, in any position of the camera in the space, at the moment of the image capture, the luminous ray reflected by the point (x,y,z) describes a straight line until the space position of the optical center of the camera.

The DLT method uses the "Collinearity Equation" to express the relation between the image coordinates (u,v) and its respective real ones (x,y,z) in the space, as it shown in Eq. (1).

$$\begin{aligned} xL_1 + yL_2 + zL_3 + L_4 - uxL_9 - uyL_{10} - uzL_{11} &= u \\ xL_5 + yL_6 + zL_7 + L_8 - vxL_9 - vyL_{10} - vzL_{11} &= v \end{aligned} \tag{1}$$

Coefficients L_1 to L_{11} are the DLT calibration parameters, which correlate the real coordinates of a point in the space (x,y,z) with its respective image coordinate (u,v). It is verified that each real point and its respective point in the image generates a pair of equations expressed in Eq. (1). As the number of unknowns is equal to 11 (parameters DLT), at least 6 calibration points (12 equations) become necessary to obtain coefficients "L".

The set of equations that composes Eq. (1) can be expressed in matrix form for n points, given by Eq. (2). This system of linear equations cannot be directly resolved, since, it is over-determined, which means that the number of lines is higher than number of columns.

$$\begin{bmatrix} x_1 & y_1 & z_1 & 1 & 0 & 0 & 0 & 0 & -u_1x_1 & -u_1y_1 & -u_1z_1 \\ 0 & 0 & 0 & 0 & x_1 & y_1 & z_1 & 1 & -v_1x_1 & -v_1y_1 & -v_1z_1 \\ & & & & & & & \vdots & & & \\ x_n & y_n & z_n & 1 & 0 & 0 & 0 & 0 & -u_nx_n & -u_ny_n & -u_nz_n \\ 0 & 0 & 0 & 0 & x_n & y_n & z_n & 1 & -v_nx_n & -v_ny_n & -v_nz_n \end{bmatrix} \begin{bmatrix} L_1 \\ L_2 \\ \vdots \\ L_{10} \\ L_{11} \end{bmatrix} = \begin{bmatrix} u_1 \\ v_1 \\ \vdots \\ u_n \\ v_n \end{bmatrix} \tag{2}$$

This problem can be solved using the least-squares method, minimizing the errors. The application of the least-squares method in Eq. (2) can be represented by Eq. (3).

$$A_{2n\,x\,11}.L_{11\,x\,1} = B_{2n\,x\,1} \tag{3}$$

Multiplying both sides of Eq. (3) for the transposed of matrix A, it will result in Eq. (4).

$$C_{11x11}.L_{11x1} = D_{11x1} \tag{4}$$

Equation (4) represents the form by which the calibration coefficients can be obtained (L_n). However, the formulation presented in Eq. (1) cannot directly be used for the reconstruction. This occurs because the real coordinates (x,y,z) are not easily put into evidence.

Manipulating again Eq. (1) to put in evidence the coordinates (x,y,z), the following equation is generated:

$$\begin{bmatrix} L_1^{(1)} - u^{(1)}L_9^{(1)} & L_2^{(1)} - u^{(1)}L_{10}^{(1)} & L_3^{(1)} - u^{(1)}L_{11}^{(1)} \\ L_5^{(1)} - v^{(1)}L_9^{(1)} & L_6^{(1)} - v^{(1)}L_{10}^{(1)} & L_7^{(1)} - v^{(1)}L_{11}^{(1)} \end{bmatrix} \begin{bmatrix} x \\ y \\ z \end{bmatrix} = \begin{bmatrix} u^{(1)} - L_4^{(1)} \\ v^{(1)} - L_8^{(1)} \end{bmatrix} \tag{5}$$

This generated system is indeterminate, since the number of equations is smaller than the number of unknowns. To solve this system, it is necessary to increase the number of cameras (m). Thus, the system can be written in the following form:

$$\begin{bmatrix} L_1^{(1)} - u^{(1)}L_9^{(1)} & L_2^{(1)} - u^{(1)}L_{10}^{(1)} & L_3^{(1)} - u^{(1)}L_{11}^{(1)} \\ L_5^{(1)} - v^{(1)}L_9^{(1)} & L_6^{(1)} - v^{(1)}L_{10}^{(1)} & L_7^{(1)} - v^{(1)}L_{11}^{(1)} \\ & \vdots & \\ L_1^{(m)} - u^{(m)}L_9^{(m)} & L_2^{(m)} - u^{(m)}L_{10}^{(m)} & L_3^{(m)} - u^{(m)}L_{11}^{(m)} \\ L_5^{(m)} - v^{(m)}L_9^{(m)} & L_6^{(m)} - v^{(m)}L_{10}^{(m)} & L_7^{(m)} - v^{(m)}L_{11}^{(m)} \end{bmatrix} \begin{bmatrix} x \\ y \\ z \end{bmatrix} = \begin{bmatrix} u^{(1)} - L_4^{(1)} \\ v^{(1)} - L_8^{(1)} \\ \vdots \\ u^{(m)} - L_4^{(m)} \\ v^{(m)} - L_8^{(m)} \end{bmatrix} \tag{6}$$

or

$$E_{2mx3}.R_{3x1} = F_{2mx1} \tag{7}$$

where m is the number of cameras and must be higher or equal to 2.

Equation (6) results in an over-determined system, which can be resolved by applying again the least-square method. The new equation can be written as:

$$G_{3x3}.R_{3x1} = H_{3x1} \tag{8}$$

Equation (8) allows that, knowing the coordinates (u,v) of the same point in the images generated by several cameras (at least two cameras), and the calibration coefficients "L" for each one of the cameras, it becomes possible to obtain the real coordinates (x,y,z) of the point.

If the movement of the structure occurs in 2D, Eq. (1) can be simplified, considering z = 0. Thus, the new equation can be written as:

$$\begin{aligned} xL_1 + yL_2 + L_3 - uxL_7 - uyL_8 &= u \\ xL_4 + yL_5 + L_6 - vxL_7 - vyL_8 &= v \end{aligned} \tag{9}$$

The set of equations for "n" calibration points can be written in the following form:

$$\begin{bmatrix} x_1 & y_1 & 1 & 0 & 0 & 0 & -u_1x_1 & u_1y_1 \\ 0 & 0 & 0 & x_1 & y_1 & 1 & -v_1x_1 & -v_1y_1 \\ & & & & \vdots & & & \\ x_n & y_n & 1 & 0 & 0 & 0 & -u_nx_n & -u_ny_n \\ 0 & 0 & 0 & x_n & y_n & 1 & -v_nx_n & -v_ny_n \end{bmatrix} \begin{bmatrix} L_1 \\ L_2 \\ \vdots \\ L_7 \\ L_8 \end{bmatrix} = \begin{bmatrix} u_1 \\ v_1 \\ \vdots \\ u_n \\ v_n \end{bmatrix} \tag{10}$$

The reconstruction process can be directly performed by the image of only one camera using the following equation:

$$\begin{bmatrix} L_1^{(1)} - u^{(1)}L_7^{(1)} & L_2^{(1)} - u^{(1)}L_8^{(1)} \\ L_4^{(1)} - v^{(1)}L_7^{(1)} & L_5^{(1)} - v^{(1)}L_8^{(1)} \end{bmatrix} \begin{bmatrix} x \\ y \end{bmatrix} = \begin{bmatrix} u^{(1)} - L_3^{(1)} \\ v^{(1)} - L_6^{(1)} \end{bmatrix} \tag{11}$$

However, to minimize errors in the values of the real coordinates (x,y), this process can be extended to several cameras:

$$\begin{bmatrix} L_1^{(1)} - u^{(1)}L_7^{(1)} & L_2^{(1)} - u^{(1)}L_8^{(1)} \\ L_4^{(1)} - v^{(1)}L_7^{(1)} & L_5^{(1)} - v^{(1)}L_8^{(1)} \\ \vdots & \vdots \\ L_1^{(m)} - u^{(m)}L_7^{(m)} & L_2^{(m)} - u^{(m)}L_8^{(m)} \\ L_4^{(m)} - v^{(m)}L_7^{(m)} & L_5^{(m)} - v^{(m)}L_8^{(m)} \end{bmatrix} \begin{bmatrix} x \\ y \end{bmatrix} = \begin{bmatrix} u^{(1)} - L_3^{(1)} \\ v^{(1)} - L_6^{(1)} \\ \vdots \\ u^{(m)} - L_3^{(m)} \\ v^{(m)} - L_6^{(m)} \end{bmatrix} \tag{12}$$

In a similar way, the solution of Eq. (12) can also be obtained by applying the least-square method. It must be reminded that the coefficients "L" in Eq. (12) must be calculated for each camera.

In the ISP, the calibration parameters (L_n) are obtained by putting the collected data in the calibration routine into Eq. (2) or Eq. (10). With the values of the calibration parameters, the real coordinates (x and y for 2D or x, y and z for 3D) and consequently, the displacements of the structure can be easily determined, using the coordinates u and v of each interest points.

2.2. Experimental Apparatus

For the dynamic experimental analysis of a clamped-free slender column under self-weight, a special device was developed, as shown in Fig. 1. This apparatus is composed by the following items:

(a) An analogical video camera.
(b) A personal computer with the ISP.
(c) A special illumination system composed with light bulbs without oscillation, with the purpose of keeping a uniform illumination on the object to be analyzed.
(d) A metallic sheet of brass representing a slender column with width b = 9.0 cm; thickness h = 0.45 mm; load per unit length (self-weight) q = 3.43 N/m; Young Modulus E = 123257 MPa; critical length l_{cr} = 56.44 cm and variable length (30 – 70cm).

For this experimental analysis, a black color background, illustrated in Fig. 1, was used in order to minimize the problems found in tests with white color background. The advantage of this strategy is to facilitate the image processing and, mainly, to eliminate the shades projected on the background by the column.

In this analysis, to represent the interest points, small white color rectangular adhesives of negligible mass were used as markers. These adhesives were placed along the length of the columns and on the background, helping the calibration process. These markers can be seen in Fig. 1.

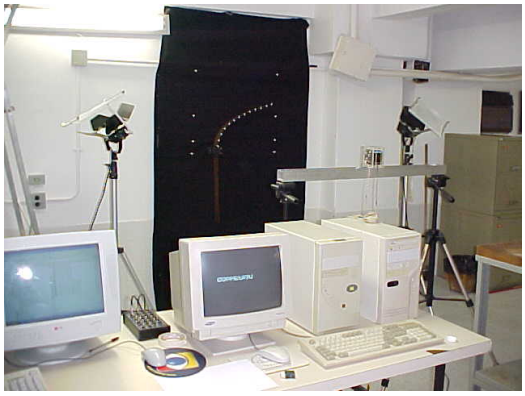

Figure 1. Experimental apparatus used in the analysis.

To allow the analysis of columns with lengths above the critical, a pulley was added to the experimental apparatus, as illustrated in Fig. 2. In this pulley a nylon wire was placed. This wire had an extremity fixed on a small object with negligible mass located on the top of the column and another one fixed on the wall. This way, the column remained in its initial position until the wire was cut, beginning the falling movement of the column.

In this experimental assay two different configurations of the column were analyzed: compressed and tensioned. For both configurations the natural frequencies and the damping ratios for the first normal mode of vibration for different column lengths were obtained.

For the compressed configuration, the columns with lengths smaller than the critical one were excited through small lateral impacts. The higher ones were released, cutting the nylon wire, performing a rough falling movement and then, exhibiting a reply in free vibration. In the tensioned configuration, the columns were excited only with small lateral impacts for all lengths. The dynamic responses were obtained through the ISP. The assays were performed using the following column lengths: 30, 40, 50, 60 and 70 cm. Figure 3 shows, for some column lengths, in both configurations, the disposal of the markers used in the calibration, located in the background, and in the structure. From these markers, the developed computational vision system obtained the responses of coordinates x and y along the time, for each one of the analyzed columns.

Figure 2. Pulley used in the experimental apparatus.

In Fig. 3a, it is also possible to observe that the calibration between the compressed columns was different. The calibration needed to be changed to keep the structure motion in the region delimited by the markers. In Fig. 3b, for tensioned columns, it was not necessary to make any modification in the calibration, since the motion of the column did not surpass the limits established by the markers.

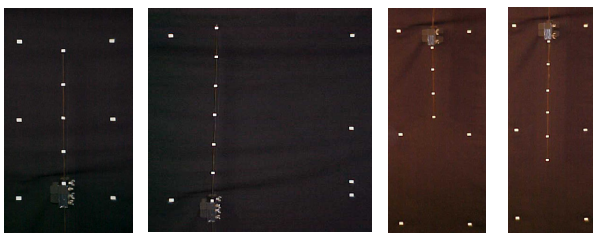

(a) Compressed (b) Tensioned

Figure 3. Disposal of the markers used in the calibration.

In these assays, the acquisition mode used by the analogical video camera to capture the images was the field mode. Although this mode introduces inaccuracy in the analysis, it presents, as a main advantage, a higher frequency of acquisition (60Hz). This frequency became essential for the analysis of the columns with lengths above the critical, mainly in the first instants, when the column exhibited a high speed.

It must be emphasized that, for the attainment of the natural frequency and the damping ratio, these first instants have not been taken into account.

3. Results and Comments

With the use of the ISP, the dynamic responses of coordinates x and y, belonging to the markers that were put along the column, were determined for both column configurations and for different lengths. Figure 4 illustrates the responses of coordinates x (a) and y (b) belonging to the marker put on the top of the compressed column with l = 60 cm. From these responses, it was possible to determine the natural frequencies and the damping ratios for the first normal mode of vibration for different lengths of the clamped-free brass column. For the evaluation of the damping ratios, the decay logarithmic method has been used.

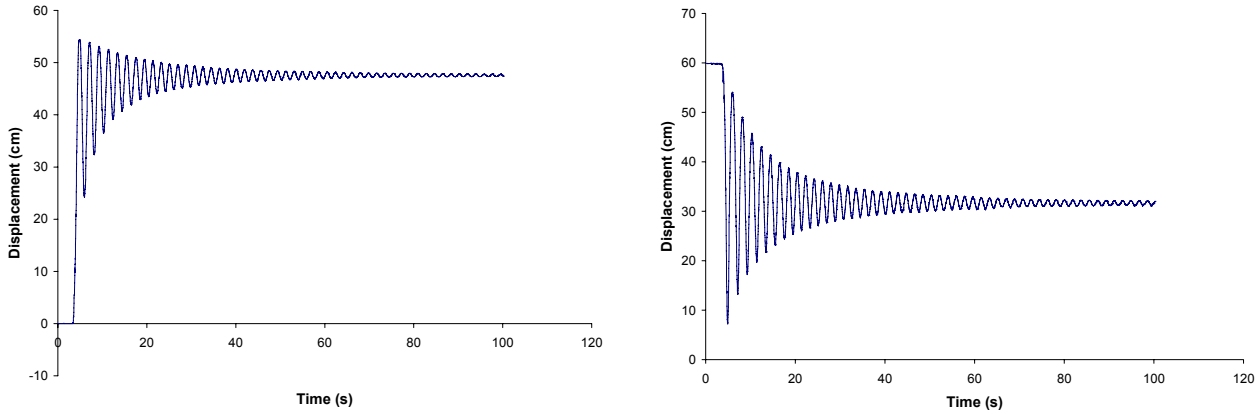

(a) Response of Coordinate x (b) Response of Coordinate y

Figure 4. Dynamic responses of coordinates x and y belonging to the marker put on the top of the column.

Figure 5 shows the quadratic variation of the smallest experimental natural frequency for increasing column lengths for compressed and tensioned configurations.

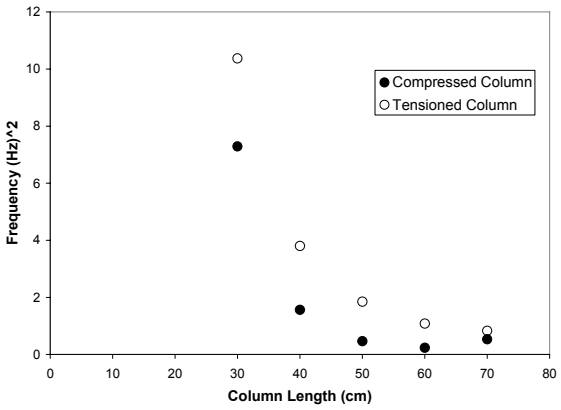

Figure 5. Quadratic variation of the smallest experimental natural frequency for increasing column lengths.

In Fig. 5, it can be observed that, as the length increases, the frequency value decreases for both column configurations. If the column was perfect, the frequency would be null in the critical length. After the buckling, the value of the smallest natural frequency increases. It can also be evidenced that the values of the frequencies for the tensioned column are higher than the values of the compressed column. This is related to the fact that the compressed column suffers a reduction in its stiffness, due to the influence of the self-weight.

In Fig. 6, the experimental natural frequencies obtained in this study for (a) compressed and (b) tensioned columns, are compared with the theoretical ones. These theoretical frequencies were obtained using Eq. (13),

$$\omega_1 = 0.00009755256162 sqrt\left(\overline{m}\left(0.522398204\times10^{9} ql^{3} + 0.3088478529\times10^{11} EI - 1\sqrt{0.1276350973\times10^{18} q^{2} l^{6} + 0.2106761186\times10^{20} EIql^{3} + 0.8750008982\times10^{21} EI^{2}}\right)\right) / \overline{m} l^{2} \quad (13)$$

where E= 123257 MPa; I (Moment of Inertia)= 6.389 x 10^{-13}m^4; $\overline{m}$ (mass per unit length)= 0.350 Kg/m; q= (±)3.43 N/m and l variable (30 – 70 cm).

The expression shown in Eq. 13 was deduced taking into account the self–weight, using Ritz's Energy Method (Jurjo, 2001).

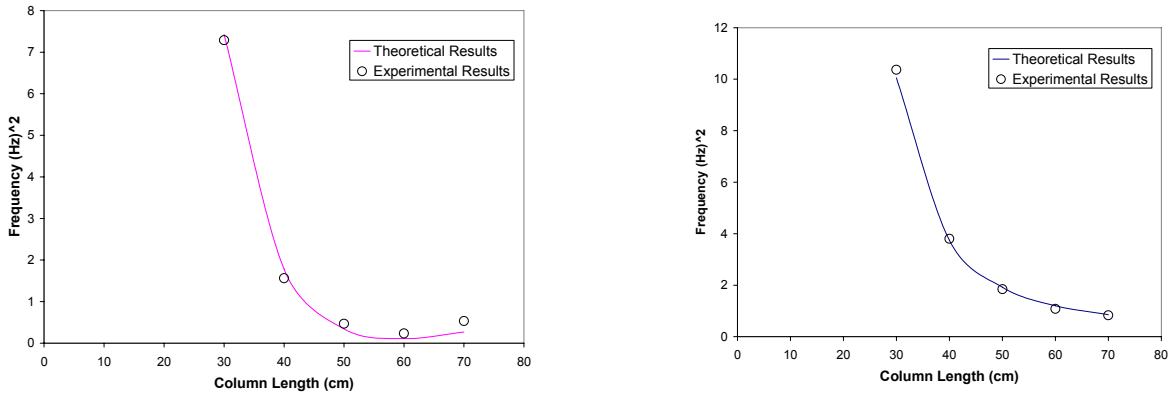

(a) Compressed Column (b) Tensioned Column

Figure 6. Quadratic variation of the experimental and theoretical natural frequencies for increasing column lengths.

From Fig. 6, it can be concluded, for the compressed columns, that this kind of behavior is characteristic of structures susceptible to buckling, where the natural frequencies decrease with the increase of the load and the natural frequency becomes null when the load is critical. The small differences between the theoretical and experimental results, around the critical configuration, are due to the small initial imperfections. It is also observed that the experimental frequency approaches to zero near the critical configuration, but increases again. This way, the column starts to vibrate around a symmetric stable post-buckling path, being its frequency proportional to the effective stiffness of the column along to the post–critical path. For tensioned columns, the frequency decreases with the increase of the length. It can also be observed that the probable value of the critical length is higher than the compressed column. This fact occurs due to the influence of self–weight, which increases the stiffness of the tensioned column. An excellent comparison is verified between the experimental and theoretical results. This shows the efficiency of the computational vision system, based on the Image–Sensor Program, developed in this study.

In Fig. 7, it is shown, for the compressed and tensioned configurations, the damping ratios for: (a) increasing column lengths and (b) increasing natural frequencies.

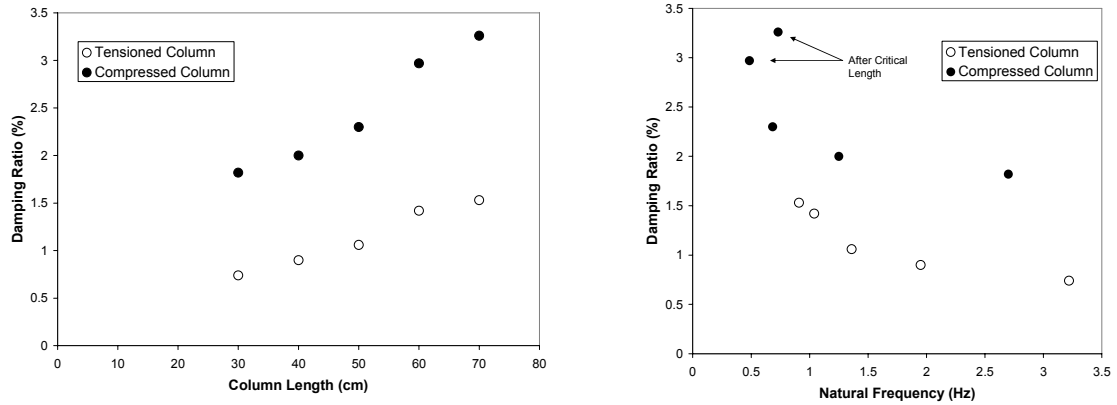

(a) Increasing column lengths (b) Increasing natural frequencies

Figure 7. Damping ratios for different lengths of tensioned and compressed columns.

In Fig. 7, for increasing lengths, it can be observed that the values of the damping ratios for tensioned column are smaller than the values for the compressed column. An increase in the value of the damping ratio for compressed column lengths above the critical value (l_{cr}= 56.44cm) is also observed. This behavior was already expected, because

previous assays with compressed columns presented this exactly same kind of behavior. Analyzing Fig. 7, for increasing frequencies, it can be noticed that while the natural frequency increases, the damping ratio decreases in a non-linear manner for column lengths smaller than the critical value. For column lengths higher than the critical value, the damping ratio and the natural frequency increase together, as can be seen in this figure, for the case of compressed columns.

4. Conclusions

In this paper, an alternative experimental methodology, based on the digital image processing techniques, has been used to study the dynamic behavior of a clamped-free thin-walled column under self–weight, with the intention to test the viability of this methodology in obtaining the dynamic displacements in structures that cannot be monitored with conventional sensors.

In order to do so, dynamic experimental assays were performed, where it can be verified an excellent correlation between the experimental results obtained with the use of image – Sensor Program and the theoretical ones.

It this study, it was evidenced that the values of the natural frequencies for the tensioned column are higher than the values for the compressed column, due to the fact that the tensioned column suffered an increase in its stiffness. Therefore, the values of the damping ratios for the tensioned column were smaller than the values for the compressed column. An increase in the value of the damping ratio for compressed column lengths above the critical value (l_{cr} = 56,44 cm) was also observed. From the analysis of the damping ratios with the natural frequencies, it was observed that the natural frequency increases while the damping ratio decreases in a non-linear manner for column lengths smaller than the critical value. For superior lengths, the damping ratio tends to rise with the increase of the natural frequency.

The proposed methodology represents an advance in the monitoring of structures that cannot be instrumented with conventional sensors, as in the case of the scale reduced models, which could have the responses of their behavior affected by the introduction of these sensors.

Another advantage of the developed vision system is the capacity of measuring dynamic displacements in several points of the structure, providing a better structural identification.

This computational vision system could also be used in structures monitored by conventional sensors, providing a reduction in the instrumentation of the assay.

Another benefit is related to the low cost of the developed system in comparison with the conventional and similar systems found in the market.

All the results obtained in this study prove the accuracy and applicability of the developed experimental methodology, based on the digital image processing techniques and the DLT method, through the use of the Image-Sensor program, for this kind of experimental dynamic analysis.

5. References

Abdel-Aziz, Y. I., Karara, H. M., 1971, “Direct linear transformation from comparator coordinates into object space coordinates in close-range photogrammetry”, Proceedings of the Symposium on Close-Range Photogrammetry, Falls Church, VA: American Society of Photogrammetry, pp. 1-18.

Barros, R.M.L., Brenzikofer, R., Leite, N.J., Figueroa, P.J., 1999, “Desenvolvimento e Avaliação de um Sistema para Análise Cinemática Tridimensional de Movimentos Humanos”, Revista Brasileira de Engenharia Biomédica, Vol.15, pp. 79 – 86.

Chen, L., Armstrong, C. W., Raftopoulos, D. D., 1994, “An investigation on the accuracy of three-dimensional space reconstruction using the direct linear transformation technique”, J. Biomechanics, Vol. 27, pp. 493-500.

Haralick, R. M. and Shapiro, L. G, 1993, “Computer and Robot Vision”, Vol. 2. Addison-Wesley Publishing Company.

Jurjo, D.L.B.R., 2004a, “Desenvolvimento de um Sistema de Visão para Medição da Resposta Dinâmica de Estruturas”, Proposta de Tese de Doutorado, Programa de Engenharia Civil, COPPE/UFRJ.

Jurjo, D.L.B.R., 2004b “Análise da Estabilidade de Colunas Sujeitas ao Peso Próprio Através do Processamento de Imagens Digitais”, Seminário de Qualificação Acadêmica para Candidatos ao Doutoramento, Programa de Engenharia Civil, COPPE/UFRJ.

Jurjo, D.L.B.R., 2001, “Estabilidade de Colunas Sujeitas ao Peso Próprio”, Dissertação de Mestrado, Departamento de Engenharia Civil, PUC-RJ.

Tsai, R.Y., 1986, “An efficient and accurate camera calibration technique for 3D machine vision”, Proceedings of IEEE Conference on Computer Vision and Pattern Recognition, Miami Beach, Florida, USA, pp. 364-374.

6. Responsibility notice

The authors are the only responsible for the printed material included in this paper.